Brighter Near-IR Emission of Single-walled Carbon Nanotubes Modified with a Cross-linked Polymer Coating

Journal:	*ChemComm*
Manuscript ID	CC-COM-04-2019-002712.R1
Article Type:	Communication

COMMUNICATION

Brighter Near-IR Emission of Single-walled Carbon Nanotubes Modified with a Cross-linked Polymer Coating

Received 00th January 20xx,
Accepted 00th January 20xx

DOI: 10.1039/x0xx00000x

Yukiko Nagai,[a] Masako Yudasaka,[b] Hiromichi Kataura,[b] and Tsuyohiko Fujigaya*[a,c,d]

Photoluminescence (PL) in the near-infrared (NIR) region is an attractive feature of single-walled carbon nanotubes (SWNTs). In this study, we investigated the effect of the chemical structure of the cross-linked polymer coating of polymer-coated SWNTs on the NIR PL emission intensity. We found that brighter NIR emission can be achieved using a more hydrophobic polymer coating.

Near-infrared (NIR) emission is useful for bioimaging and biosensing owing to relatively weak absorption of the NIR region in the body.[1, 2] Single-walled carbon nanotubes (SWNTs), especially semiconducting-type SWNTs, are a unique material with strong photon absorption[3, 4] and emission[5, 6] in the NIR region, and various studies on utilizing NIR emission have been performed.[7-9] One issue for achieving strong NIR emission is isolation of the SWNTs from the strong agglomerates to avoid quenching by metallic-type SWNTs. To realize stable isolation, physical modification[10, 11] of SWNTs with surfactants is often performed in an aqueous system, and it is better than chemical modification.[12] However, dynamic replacement of the dispersants can lead to detachment, resulting in SWNT aggregation.[13]

Isolation of SWNTs by cross-linked polymers has attracted attention[14-21] because the excellent dispersion stability can overcome detachment issues. We recently developed a novel method to create a very thin (~1 nm) cross-linked polymer layer on the SWNT surface without introducing chemical defects, which we called the carbon nanotube (CNT) micelle polymerization method (Scheme 1).[22] This method is characterized by quantitative coating yield,[22] monomer versatility,[23] and additional functionalization.[24, 25] However, the PL intensity of SWNTs coated with a cross-linked polymer is not as strong as that of the SWNTs dispersed in surfactants.

In this study, we investigated the effect of the coating conditions and chemical structure of the cross-linked polymer coating on the PL intensity. In addition, the type of surfactant, centrifugation conditions, and monomer structure were optimized. We found that the hydrophobicity of the monomer is crucially important for the PL intensity of the polymer-coated SWNTs. In addition, brighter PL emission was achieved using *N*-ethylacrylamide (EAA) as the coating monomer compared with SWNTs dispersed by a conventional biosurfactant.

Scheme 1 Schematic of CNT micelle polymerization.

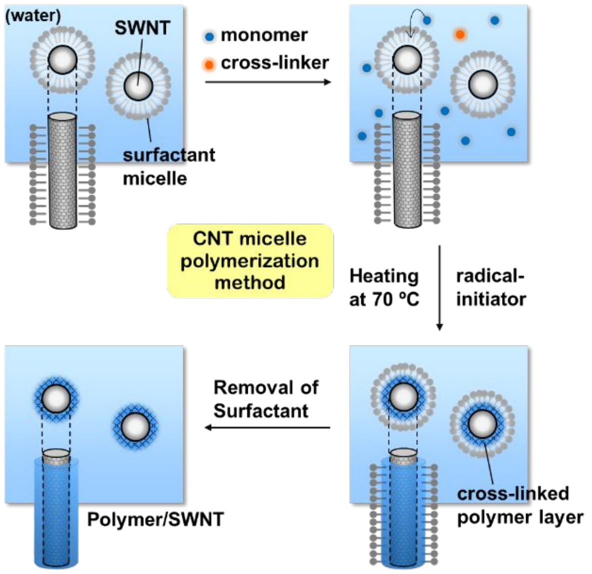

Coating SWNTs with the cross-linked polymers was performed based on a reported procedure using an aqueous surfactant dispersion with *N*-isopropylacrylamide (NIPAM),

---

[a] *Department of Applied Chemistry, Graduate School of Engineering, Kyushu University, 744 Motooka, Nishi-ku, Fukuoka 819-0395, Japan. E-mail: fujigaya.tsuyohiko.948@m.kyushu-u.ac.jp*
[b] *Nanomaterials Research Institute, National Institute of Advanced Industrial Science and Technology (AIST), Higashi 1-1-1, Tsukuba, Ibaraki 305-8565, Japan.*
[c] *International Institute for Carbon Neutral Energy Research (WPI-I²CNER), Kyushu University, Fukuoka 819-0395, Japan.*
[d] *Center for Molecular Systems (CMS), Kyushu University, 744 Motooka, Nishi-ku, Fukuoka 819-0395, Japan.*

† Electronic Supplementary Information (ESI) available. See DOI: 10.1039/x0xx00000x

ammonium persulfate, and *N,N′*-methylenebisacrylamide as the monomer, radical initiator, and cross-linker, respectively.[26, 27] We previously used sodium dodecyl sulfate (SDS) as the surfactant. However, we used sodium dodecyl benzenesulfonate (SDBS) in this study because it is known to disperse large-diameter SWNTs[28] (Fig. S1, ESI†). In addition, in our previous study,[29] we used 0.2 wt% SDS solution (6.94 mM), which is slightly less than the critical micelle concentration (CMC) of SDS (8.35 mM). However, in this study, we used 2.0 wt% SDBS solution (57.4 mM), which is greater than the CMC of SDBS (1.6 mM),[30] to facilitate isolation[31] (Fig. S2, ESI†).

After polymerization and repeated filtration and centrifugation (600,000 g) to remove SDBS and NIPAM polymer (PNIPAM) particles, a faintly black dispersion (Fig. 1a) containing SWNTs wrapped in PNIPAM (PNIPAM/SWNTs) was obtained. Removal of SDBS was confirmed by X-ray photoelectron spectroscopy (XPS) because of the absence of the S 2p peak from the sulfonate group (Fig. S3, ESI†). The PNIPAM/SWNT dispersion was stable in aqueous solution even after SDBS removal, indicating formation of a stable coating of cross-linked PNIPAM on the SWNTs. Based on the comparable intensities of the initial SWNT dispersion in SDBS and the PNIPAM/SWNT dispersion (Fig. S4, ESI†), PNIPAM/SWNTs were obtained in quantitative yield.[22]

The PL contour plot of the PNIPAM/SWNT dispersion before centrifugation at 600,000 g is shown in Fig. 1b, where the chiral indices are expressed as (m, n). Interestingly, the PL was enhanced after centrifugation, especially for SWNTs with relatively large diameter, such as (8, 6) and (8, 7) (Fig. 1c). The pH of the dispersion before centrifugation was low (pH = 4.5), probably because of dissociation of H^+ from the ammonium ion ($NH_4^+ \rightarrow NH_3 + H^+$). However, the pH of the dispersion after centrifugation increased to pH = 6.9, probably because of dilution of the solution upon repeated centrifugation and replacement of the supernatant with fresh water. Such diameter-selective quenching and recovery of the PL is often observed with hole doping by acid and electron doping by alkaline, respectively, in which a larger SWNT with a higher HOMO level preferentially responds to the process.[32, 33] It is important to note that the PL intensity in Fig. 1c is much higher than that of the PNIPAM/SWNT dispersion prepared in 0.2 wt% SDS solution at a comparable concentration (Fig. S5, ESI†).

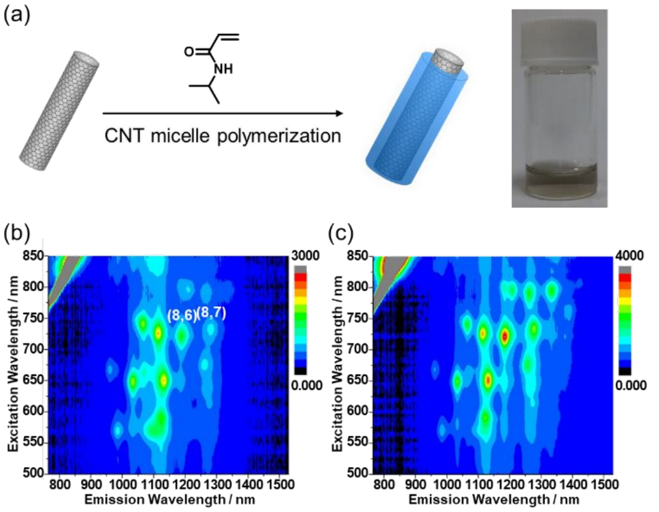

Fig. 1 (a) CNT micelle polymerization using NIPAM (left) and a photograph of the PNIPAM/SWNT dispersion after centrifugation at 600,000 g (right). (c) and (d) PL contour plots of the PNIPAM/SWNT dispersion before and after centrifugation at 600,000 g, respectively.

Given the importance of initial isolation of the SWNTs with the solution pH, we investigated the effect of the monomer structure on the PL intensity of the SWNTs. The four monomers EAA, *N-tert*-butylacrylamide (TBA), *N,N*-diethylacrylamide (DEAA), and *N,N*-dimethylacrylamide (DMAA) were used to prepare poly(EAA) (PEAA)/SWNTs (Fig. S6a, ESI†), poly(TBA) (PTBA)/SWNTs (Fig. S6b, ESI†), poly(DEAA) (PDEAA)/SWNTs (Fig. S6c, ESI†), and poly(DMAA) (PDMAA)/SWNTs (Fig. S6d, ESI†), respectively. All of the monomers produced very stable aqueous dispersions after removal of SDBS, indicating formation of the cross-linked polymers around the SWNTs. As the matter of fact, Raman D-band intensity at 1295 cm^{-1} with respective to that of the G-band at 1595 cm^{-1} (G/D ratio), practical indicator of the defect content in a SWNT surface,[34, 35] was almost unchanged during the polymerization (Fig. S7, ESI†).

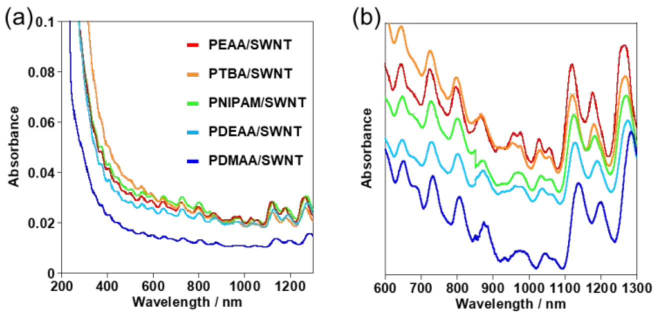

Fig. 2 (a) Absorption spectra of the PNIPAM/SWNTs (light green), PEAA/SWNTs (red), PTBA/SWNTs (orange), PDEAA/SWNTs (light blue), and PDMAA/SWNTs (blue) after purification. (b) Magnification of the range 600–1300 nm. The spectra are shifted for clear comparison.

The absorption spectra of the PNIPAM/SWNTs, PEAA/SWNTs, PTBA/SWNTs, PDEAA/SWNTs, and PDMAA/SWNTs after purification are shown in Fig. 2a. Several peaks owing to the interband transition between S_{11} (900–1300 nm) and S_{22} (600–900 nm) of different chiral indices are clearly observed in the NIR region. The wavelength peaks shifted depending on the type of monomer used for polymerization (Fig. 2b). The PL contour plots of the SWNT hybrids are shown in Fig. 3. For all of the dispersions, there are clear PL spots originating from the isolated SWNTs.

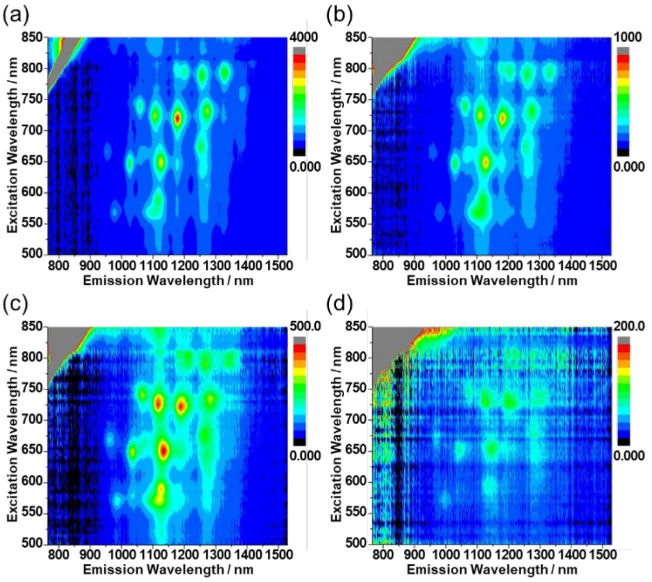

Fig. 3 PL contour plots of the (a) PEAA/SWNTs, (b) PTBA/SWNTs, (c) PDEAA/SWNTs, and (d) PDMAA/SWNTs after purification.

The PL intensity of (8, 6) normalized by the absorption intensity of the (8, 6) SWNTs is plotted as a function of the absorption peak wavelength in Fig. 4. Remarkably, there is a strong linear relationship between the normalized PL intensity and the absorption peak wavelength. A more hydrophobic environment induces a blue shift of the absorption owing to reduction of the dielectric constant.[36] In addition, it has been reported that a hydrophobic environment is preferable for bright PL emission because oxidation of the SWNTs by H_2O can be prevented.[36] Therefore, the good linearity in Fig. 4 strongly indicates that the hydrophobicity of the SWNT environment can be controlled by changing the chemical structure of the monomer, and a more hydrophobic environment results in brighter PL emission of the SWNTs. Other chiral indices, such as (7, 6), also show similar linearity (Fig. S8, ESI†).

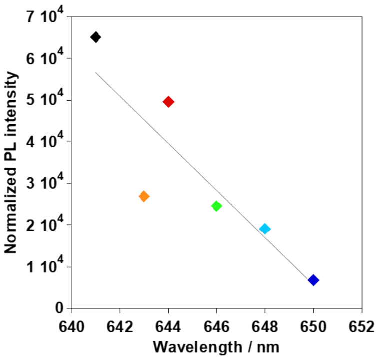

Fig. 4 Plot of the normalized PL intensity of the (8, 6) SWNTs for the SDBS/SWNTs (black), PNIPAM/SWNTs (light green), PEAA/SWNTs (red), PTBA/SWNTs (orange), PDEAA/SWNTs (light blue), and PDMAA/SWNTs (blue) as a function of their absorption peak wavelength after purification.

Photos of the dispersions of the SWNTs coated by cross-linked polymers taken with a NIR camera (InGaAs-array video camera, NIRvana 640ST, Princeton Instruments, Trenton, NJ, USA) are shown in Fig. 5a. SWNTs dispersed by phospholipid polyethylene glycol (PLPEG) are used as the reference because PLPEG-dispersed SWNTs are often used for NIR imaging in mice.[9] The PNIPAM/SWNTs, PEAA/SWNTs, PTBA/SWNTs, PDEAA/SWNTs, and PDMAA/SWNTs showed PL intensities of 17,956, 30,008, 19,408, 10,711, and 1776 (N = 3), respectively (Fig. 5a). The PEAA/SWNTs coated with the most hydrophobic gel showed the highest PL intensity (Fig. 4). Importantly, the PEAA/SWNTs showed about 1.5 times brighter PL than the PLPEG/SWNTs (Fig. 5b). Therefore, the PEAA/SWNT hybrid is considered to be a promising material for imaging applications *in vivo* considering its characteristic dispersion stability and bright PL emission.

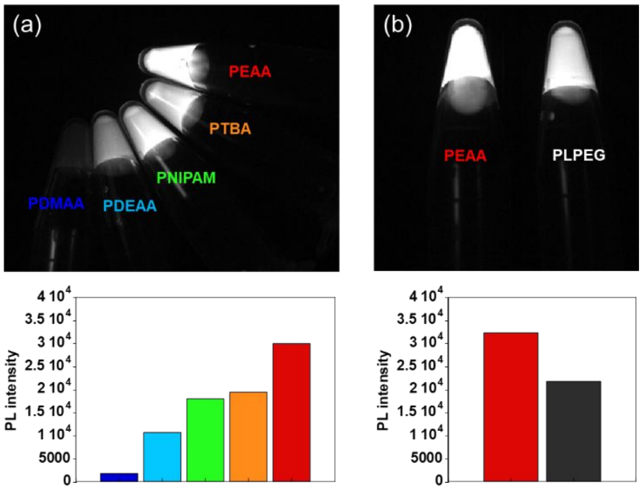

Fig. 5 NIR fluorescence images and intensities of the samples. (a) PNIPAM/SWNTs (light green), PEAA/SWNTs (red), PTBA/SWNTs (orange), PDEAA/SWNTs (light blue), and PDMAA/SWNTs (blue). (b) PEAA/SWNTs (red) and PLPEG-dispersed SWNTs (gray).

In conclusion, we have investigated the effect of the chemical structure of the cross-linked polymer of polymer-coated SWNTs on the PL intensity. We found that more hydrophobic monomers produce brighter PL emission after polymerization. In addition, the PEAA/SWNTs showed brighter PL emission than the PLGEG/SWNTs typically used for biological applications. By taking advantage of the monomer versatility of this coating method, development of a new hydrophobic monomer with active sites for post-modification will provide SWNT hybrids with bright NIR PL and additional functionality, such as active targeting by ligands, which is promising for NIR imaging and therapy *in vivo*.

This study was supported in part by the Nanotechnology Platform Project from the Ministry of Education, Culture, Sports, Science, and Technology, Japan, KAKENHI (Nos. JP16K14084 and JP16H06056) from the Japan Society for the Promotion of Science, and PRESTO (No. JPMJPR15R6) from Japan Science and Technology Agency (JST), Japan. We thank Edanz Group (www.edanzediting.com/ac) for editing a draft of this manuscript.

Conflicts of interest

There are no conflicts to declare.

Notes and references

1. K. Welsher, Z. Liu, S. P. Sherlock, J. T. Robinson, Z. Chen, D. Daranciang and H. Dai, *Nat. Nanotech.*, 2009, **4**, 773-780.
2. A. L. Antaris, H. Chen, S. Diao, Z. Ma, Z. Zhang, S. Zhu, J. Wang, A. X. Lozano, Q. Fan and L. Chew, *Nat. Comm.*, 2017, **8**, 15269.
3. E. S. Jeng, A. E. Moll, A. C. Roy, J. B. Gastala and M. S. Strano, *Nano Lett.*, 2006, **6**, 371-375.
4. R. Weissleder, *Nat. Biotechnol.*, 2001, **19**, 316-317.
5. S. M. Bachilo, M. S. Strano, C. Kittrell, R. H. Hauge, R. E. Smalley and R. B. Weisman, *Science*, 2002, **298**, 2361-2366.
6. M. J. O'connell, S. M. Bachilo, C. B. Huffman, V. C. Moore, M. S. Strano, E. H. Haroz, K. L. Rialon, P. J. Boul, W. H. Noon and C. Kittrell, *Science*, 2002, **297**, 593-596.
7. Y. Yomogida, T. Tanaka, M. Zhang, M. Yudasaka, X. Wei and H. Kataura, *Nat. Comm.*, 2016, **7**, 12056.
8. M. Yudasaka, Y. Yomogida, M. Zhang, T. Tanaka, M. Nakahara, N. Kobayashi, Y. Okamatsu-Ogura, K. Machida, K. Ishihara and K. Saeki, *Sci. Rep.*, 2017, **7**, 44760.
9. M. Yudasaka, Y. Yomogida, M. Zhang, M. Nakahara, N. Kobayashi, T. Tanaka, Y. Okamatsu-Ogura, K. Saeki and H. Kataura, *Sci. Rep.*, 2018, **8**.
10. T. Fujigaya and N. Nakashima, *Polymer J.*, 2008, **40**, 577-589.
11. R. J. Chen, Y. Zhang, D. Wang and H. Dai, *J. Am. Chem. Soc.*, 2001, **123**, 3838-3839.
12. N. Karousis, N. Tagmatarchis and D. Tasis, *Chem. Rev.*, 2010, **110**, 5366-5397.
13. D. Roxbury, X. Tu, M. Zheng and A. Jagota, *Langmuir*, 2011, **27**, 8282-8293.
14. C. Roquelet, J. S. Lauret, V. Alain - Rizzo, C. Voisin, R. Fleurier, M. Delarue, D. Garrot, A. Loiseau, P. Roussignol and J. A. Delaire, *ChemPhysChem*, 2010, **11**, 1667-1672.
15. W.-C. Chen, R. K. Wang and K. J. Ziegler, *ACS applied materials & interfaces*, 2009, **1**, 1821-1826.
16. G. Clave, G. Delport, C. Roquelet, J.-S. Lauret, E. Deleporte, F. Vialla, B. Langlois, R. Parret, C. Voisin and P. Roussignol, *Chem. Mater.*, 2013, **25**, 2700-2707.
17. Y. Kang and T. A. Taton, *J. Am. Chem. Soc.*, 2003, **125**, 5650-5651.
18. T. H. Kim, C. Doe, S. R. Kline and S. M. Choi, *Adv. Mater.*, 2007, **19**, 929-933.
19. C. Thauvin, S. Rickling, P. Schultz, H. Celia, S. Meunier and C. Mioskowski, *Nat. Nanotechnol.*, 2008, **3**, 743.
20. C. d. Thauvin, A. l. Perino, E. Contal, E. Morin, P. Schultz, S. p. Meunier and A. Wagner, *J. Phys. Chem. C*, 2011, **115**, 7319-7322.
21. R. Wang, P. Cherukuri, J. G. Duque, T. K. Leeuw, M. K. Lackey, C. H. Moran, V. C. Moore, J. L. Conyers, R. E. Smalley, H. K. Schmidt, R. B. Weisman and P. S. Engel, *Carbon*, 2007, **45**, 2388-2393.
22. Y. Tsutsumi, T. Fujigaya and N. Nakashima, *RSC Adv.*, 2014, **4**, 6318-6323.
23. Y. Tsutsumi, T. Fujigaya and N. Nakashima, *Chem. Lett.*, 2015, **45**, 274-276.
24. Y. Nagai, Y. Tsutsumi, N. Nakashima and T. Fujigaya, *J. Am. Chem. Soc.*, 2018, **140**, 8544-8550.
25. Y. Tsutsumi, T. Fujigaya and N. Nakashima, *Nanoscale*, 2015, **7**, 19534-19539.
26. Y. Hong, Z. Mao, H. Wang, C. Gao and J. Shen, *Journal of Biomedical Materials Research Part A*, 2006, **79**, 913-922.
27. J. Chang, Y. Tao, B. Wang, X. Yang, H. Xu, Y.-r. Jiang, B.-h. Guo and Y. Huang, *Polymer*, 2014, **55**, 4627-4633.
28. W. Wenseleers, I. I. Vlasov, E. Goovaerts, E. D. Obraztsova, A. S. Lobach and A. Bouwen, *Adv. Funct. Mater.*, 2004, **14**, 1105-1112.
29. T. J. McDonald, C. Engtrakul, M. Jones, G. Rumbles and M. J. Heben, *J. Phys. Chem. B*, 2006, **110**, 25339-25346.
30. T. J. McDonald, C. Engtrakul, M. Jones, G. Rumbles and M. J. Heben, *J. Phys. Chem. B*, 2006, **110**, 25339-25346.
31. M. Suttipong, N. R. Tummala, B. Kitiyanan and A. Striolo, *J. Phys. Chem. C*, 2011, **115**, 17286-17296.
32. R. K. Wang, W. C. Chen, D. K. Campos and K. J. Ziegler, *J. Am. Chem. Soc.*, 2008, **130**, 16330-16337.
33. G. Dukovic, B. E. White, Z. Zhou, F. Wang, S. Jockusch, M. L. Steigerwald, T. F. Heinz, R. A. Friesner, N. J. Turro and L. E. Brus, *J. Am. Chem. Soc.*, 2004, **126**, 15269-15276.
34. S. Bandow, A. Rao, K. Williams, A. Thess, R. Smalley and P. Eklund, *J. Phys. Chem. B*, 1997, **101**, 8839-8842.
35. V. Karachevtsev, A. Y. Glamazda, U. Dettlaff-Weglikowska, V. Kurnosov, E. Obraztsova, A. Peschanskii, V. Eremenko and S. Roth, *Carbon*, 2003, **41**, 1567-1574.
36. B. A. Larsen, P. Deria, J. M. Holt, I. N. Stanton, M. J. Heben, M. J. Therien and J. L. Blackburn, *J. Am. Chem. Soc.*, 2012, **134**, 12485-12491.

.